PHYSICAL REVIEW B VOLUME 16, NUMBER 9 1 NOVEMBER 1977

Effects of diffusion on magnetic excitations in films of yttrium iron garnet

C. Vittoria and J. H. Schelleng
Naval Research Laboratory, Washington, D.C. 20375
(Received 28 March 1977)

We have investigated the effects of a diffusion located at the yttrium iron garnet–gadolinium gallium garnet (YIG-GdGaG) interface on spin-wave excitations. We calculate at ambient temperatures that a localized or surface spin-wave mode can be excited in chemical vapor deposited but not in liquid phase epitaxy (LPE) films of YIG. This localized state can be excited for the magnetic field applied parallel but not perpendicular to the film plane, in agreement with experimental observations. The dependence of spin-wave intensities on the direction of the magnetic field, observed in LPE films, is explained in terms of a nonuniform distribution of the cubic magnetic anisotropy field at the interface.

I. INTRODUCTION

In this paper, we are investigating the effects of the diffusion layer located at the interface between single-crystal yttrium iron garnet (YIG) films and gadolinium gallium garnet (GdGaG) substrate on magnetic resonance excitations. In a finite-dimensional film there are various magnetic excitations that can occur. Magnetic excitations that quantize the in-plane dimension of the film are referred to as magnetostatic mode excitations. Magnetic excitations that quantize the dimensions normal to the film are referred to as standing spin-wave mode excitations. We will discuss the latter type of excitations. Specifically, we will consider the effects of diffusion on the excitation of surface energy states localized at the interface and on volume spin waves in both chemical vapor deposited (CVD) and liquid phase epitaxy (LPE) films.

The growth of single-crystal YIG films by either the CVD or LPE technique is a fairly recent achievment. CVD YIG films are prepared at ~1250 °C, and LPE films at ~900 °C. The process of "growing" these films at high temperatures induces a slow variation in ion concentrations near the interface.[1] The thin film geometry allows for the excitation of standing spin-wave resonance (SWR) modes. We will demonstrate that the combined effects of (i) the fact that YIG is a well-characterized material, (ii) measurements[1] of the ion profile near the interface by Auger spectroscopy, and (iii) the correlation of the ferrimagnetic resonance (FMR) with the Auger work provides us with the information required in order to propose a model for surface and volume spin-wave excitations in CVD and LPE films.

FMR studies on CVD films were first reported by Besser and Sparks *et al.*[2] Volume spin-wave modes were readily excited[2] in thin ($\lesssim 1$ μm) films of CVD YIG. With very thin CVD films ($\sim\frac{1}{3}$ μm), the volume spin-wave mode field positions deviated[3] from the n^2 law as predicted by Kittel,[4] where n is the spin-wave order number and it is an integer. It was hypothesized[3] that this deviation was due to some nonuniform distribution of M near the interface between YIG and GdGaG. By assuming[5,6] an analytical variation of M near the interface, the calculated[5,6] spin-wave field positions agreed with the observed[3] field values. This hypothesis[3] is in agreement with Auger measurements[1] of the ion concentrations near the interface where the measurements show a nonuniform distribution of magnetic ions.

A systematic and complete experimental study was carried out by Yu, Turk, and Wigen[7] on the excitation of surface states in CVD YIG films. This excitation occurs for dc magnetic fields above the main or uniform Kittel mode, whereas volume spin-wave modes occur for fields below the main line. For the magnetic field H_a applied perpendicular to the film plane, there are only excitations of volume spin-wave modes and no surface state. For other directions of $\vec{H}_a$, both surface and volume spin-wave modes are excited. It was demonstrated that the surface state was localized at the YIG-GdGaG interface. The FMR results of Yu, Turk, and Wigen[7] were analyzed in terms of a surface magnetic anistropy parameter K_s which depended on the direction of $\vec{H}_a$. It was demonstrated[7] that K_s would take on a particular value for $\vec{H}_a$ parallel to the film plane and a different value for $\vec{H}_a$ perpendicular to the film plane.

With a sensitivity of $10^{12}\Delta H$ spins, we were not able to detect surface spin waves in LPE films at room temperature. Volume spin-wave mode intensities in LPE YIG films were also weak[8] when compared with corresponding intensities in CVD YIG films,[3] but they were resolved by our spectrometer. The field positions obey the n^2 law. However, the intensity amplitude for a particular n is dependent[9] on the direction of $\vec{H}_a$. One finds that if one analyzes the LPE spin-wave intensity

data in terms of K_s, one must invoke a K_s that depends on the in-plane angle of $\vec{H}_a$. For example, with $\vec{H}_a$ in the {100} plane and parallel to one of the four equivalent ⟨100⟩ axes, K_s (for one side of the film) is deduced[9] to be a particular value and a different value for $\vec{H}_a$ parallel to one of the four equivalent ⟨110⟩ axes. This, of course, violates the basic definition of uniaxial magnetic surface energy.

Although reliable values of K_s have been obtained for YIG films and for many other different materials, the parameter K_s can at best represent indirectly or simulate the physical mechanism occurring at a surface. We are proposing a spin-pinning mechanism which does not require that magnetic properties change with the direction of $\vec{H}_a$. We will demonstrate that this mechanism is able to predict directly spin-wave excitations occurring in CVD and LPE films.

Previous models have considered variations of magnetization throughout the film and near[10] the surface in order to fit some FMR data in films. An analytical variation in magnetization was *assumed* in calculating the spinwave spectrum. In order to explain our LPE data, we *require* variations of not only the magnetization but also of the magnetic anisotropy and exchange. In this work, actual compositional variation was measured at the interface between YIG and GdGaG by Auger spectroscopy. This allowed us to deduce or calculate the variation of magnetization, magnetic anisotropy and exchange without the need of *any* assumptions regarding the properties of the YIG-GdGaG interface.

In proposing our mechanism, we made use of the Auger data[1] where the ion concentration profile of Fe, Y, Gd, and Ga at the interface was measured. The saturation magnetization M, the cubic magnetic anisotropy parameter K_1, and the exchange constant D were calculated from the concentration profile. A molecular-field theory was used to obtain M, a single-ion model[11,12] was used to obtain K_1, and D was calculated by various approximations.[13,14] This allowed us to write a general equation of motion for the moment which was valid both in bulk YIG and at the interface.

This general equation of motion for the moment can be put in the form of Schrödinger's wave equation. In doing so, we introduce an effective potential which is defined for $\vec{H}_a$ parallel to the film plane as

$$V_{\parallel}(y) \simeq H_a + 2\pi M - \frac{D}{M}\frac{\partial^2 M}{\partial y^2},$$

and for $\vec{H}_a$ perpendicular to the film plane as

$$V_{\perp}(y) = H_a - 4\pi M - \frac{D}{M}\frac{\partial^2 M}{\partial y^2}.$$

The effective potential is dependent on the coordinate y normal to the film plane, since the magnetic parameters are y dependent. For CVD films, the diffusion is wider and the effective potential gives rise to a potential "well" which resembles a Morse potential well. For H_a parallel to the film plane, the well is of sufficient depth and width to support one bound state at the interface. For H_a perpendicular to the film plane, the well is too shallow to support a bound state. It is claimed that this type of bound state corresponds to the surface spin-wave state observed experimentally by Yu, Turk, and Wigen.[7] Also, the variation in M can also effect the field position of volume spin-wave modes, as it was the case[5,6] in CVD films.

For LPE films, the diffusion is too narrow to support a localized state. However, it will be demonstrated that a small variation in K_1 alone is sufficient to induce angular variation in volume spin-wave intensities as observed experimentally.[9]

Throughout the analysis of this work, we have sacrificed some mathematical rigor in order to demonstrate the effects in a most direct way. In Sec. II we derive the equation of motion for M necessary to describe the effects. The equation of motion contains terms with coefficients which are a function of M, K_1, and D. An analysis is devised to determine these parameters at the interface from concentration profile obtained from the Auger data.[1] In Sec. III, the Auger data is presented with the corresponding values of K_1, M, and D determined from the analysis of Sec. II. Finally, the magnetic diffusion profile is used in the calculations to predict the surface state in CVD films and to determine quantitatively the anisotropy in volume spin-wave intensities. The calculations are in agreement with observed spin-wave spectra in CVD and LPE films of YIG.

II. SPIN-WAVE RESONANCE ANALYSIS

In this section, the differential equations governing the dynamics of the transverse components of the magnetization are derived. We choose the y and z directions to be perpendicular and parallel to the film plane, H_a will be applied along one of these directions. Initially, we assume a magnetically isotropic medium. We will later add the complications of magnetic anisotropy.

Starting with Landau-Lifshitz equation[15] of motion and assuming spatial variation for all components of the magnetization and no magnetic damping, the following linearized equations for the transverse rf components (m_x and m_y) of the magnetization is obtained for $\vec{H}_a$ in the film plane

$$j\Omega m_x = (a' + 4\pi M) m_y, \tag{1}$$

$$j\Omega m_y = -a' m_x, \tag{2}$$

where

$$\Omega = \omega/\gamma,$$

$$a' = H + \frac{D}{M}\frac{\partial^2 M}{\partial y^2} - D\frac{\partial^2}{\partial y^2},$$

$$H = H_a.$$

H is the internal static field, ω is the operating frequency, and $\gamma = ge/2mc$. The second and third terms in a' are the exchange fields for a spatial variation in the static and rf magnetizations. The factor D is recognized in the familiar form of $2A/M$ where A is the exchange stiffness constant. The variation of M with y near the interface can be determined from the Auger work.[1] The variation of D, M, and also of K_1 near the interface will be calculated in the next section. For calculational purposes the D term is preferred in Eqs. (1) and (2).

For H_a in the film plane, the motion of m_x and m_y is elliptical; thus, we introduce the transformations

$$m_\pm = m_x \pm jNm_y.$$

For $N \neq 1$, the locus of m_x and m_y describe an elliptical path, whereas for $N = 1$ they describe a circular path. Substituting the two transformations into Eqs. (1) and (2), we obtain

$$\Omega m_\pm = \mp a' N m_\pm, \tag{3}$$

where

$$N = (1 + 4\pi M/a')^{1/2}.$$

At high frequencies such that the resonant field $H_a > 4\pi M$, we can approximate (3) as

$$\Omega m_\pm \approx \mp (a' + 2\pi M) m_\pm. \tag{4}$$

Let us examine the validity of this approximation in the limit of no spatial variation. From Eq. (4), one obtains the dispersion

$$\Omega = H + Dk^2 + 2\pi M; \tag{5}$$

the exact dispersion is given as[16]

$$\Omega^2 = (H + Dk^2)(H + Dk^2 + 4\pi M). \tag{6}$$

For long-wavelength excitation the k^2 dependence of spin waves is still maintained in the approximate relation. However, for $k = 0$, the approximate resonant field, using Eq. (5), is 2425 Oe at X band ($\Omega = 3300$ Oe, $2\pi M = 875$ G), while Eq. (6) gives 2540 Oe. Thus, a small error occurs for the uniform mode. Equation (5) is useful at X band and higher frequencies. The advantage of using Eq. (4) is that a second-order differential equation is obtained from it instead of a fourth-order one. The approximation should also hold at the interface, since $4\pi M$ becomes a smaller factor when compared to a'.

The contribution from $(D/M)\partial^2 M/\partial y^2$ makes a' smaller. For our case, the value of a' reduces roughly by a maximum value of 10% at the interface. However, this reduction is compensated by the fact that $4\pi M$ also reduces by the same amount. Thus, we see that Eq. (4) should remain valid in the interface region for X-band frequencies and above.

For the case of $\vec{H}_a$ applied normal to the film plane, the rf demagnetizing fields can be neglected and Eqs. (1) and (2) simply become

$$j\Omega m_x = a' m_z, \tag{7}$$

$$j\Omega m_z = -a' m_x. \tag{8}$$

Writing the above equations in terms of circularly polarized fields, one gets

$$m_\pm = \mp a' m_\pm \tag{9}$$

The difference here is that the internal static field is defined as

$$H = H_a - 4\pi M,$$

where $4\pi M$ is the dc demagnetizing field. Using Eqs. (4) and (9), the corresponding differential equations for the two cases become

$$D\frac{\partial^2 m}{\partial y^2} + \left[\Omega - \left(H_a^{\parallel} + 2\pi M + \frac{D}{M}\frac{\partial^2 M}{\partial y^2}\right)\right], \quad m \cong 0., \tag{10}$$

$$D\frac{\partial^2 m}{\partial y^2} + \left[\Omega - \left(H_a^{\perp} - 4\pi M + \frac{D}{M}\frac{\partial^2 M}{\partial y^2}\right)\right], \quad m = 0. \tag{11}$$

Although we have dropped the subscripts on m, the m in Eq. (10) implies an elliptical polarization. In Eq. (11), m implies circular polarization. The applied magnetic field directions with respect to the film plane in Eqs. (10) and (11) are indicated by the superscripts on H_a.

It is recognized that Eqs. (10) and (11) are of the same form as Schrödinger's wave equation

$$\frac{\hbar^2}{2\rho}\frac{\partial^2 \psi}{\partial y^2} + (E - V)\psi = 0. \tag{12}$$

Thus, we identify an effective potential as

$$V_{\parallel} = H_a^{\parallel} + 2\pi M + \frac{D}{M}\frac{\partial^2 M}{\partial y^2} \tag{13}$$

for H_a parallel to the film plane,

$$V_{\perp} = H_a^{\perp} - 4\pi M + \frac{D}{M}\frac{\partial^2 M}{\partial y^2} \tag{14}$$

for H_a perpendicular to the film plane, and $E \equiv \Omega$. In deriving $V_{\parallel}$ and $V_{\perp}$, we made the implicit assumption that D is constant at the interface. As we shall see, the variation in D at the interface is sufficiently small enough to let us adopt this for-

malism.

Equations (13) and (14) allow us to compare directly the effective potentials for the two directions of H_a. The difference between $V_{\parallel}$ and $V_{\perp}$ is $\approx 6\pi M$. We will demonstrate that difference can account for the "anomalous" excitation of surface spin waves in CVD films.

To explain the anisotropic behavior of spin-wave intensities found[9] in LPE films of YIG we must use differential equations containing the K_1 factor. For simplicity, we will only consider the $\{100\}$ plane, since the analysis is the same for any other plane. In particular, we will be concerned with H_a parallel to the $\langle 100\rangle$ and $\langle 110\rangle$ axes and in the film plane. For the $\langle 100\rangle$ direction the a'coefficient is redefined[17] as

$$a' = (a')_{\text{isotropic}} + 2K_1/M.$$

For the $\langle 110\rangle$ direction

$$a' = (a')_{\text{isotropic}} - 2K_1/M.$$

For the $\langle 110\rangle$ axis an additional term of $3K_1/M$ must be included[17] inside the parenthesis of Eq. (1). For both directions, the second-order anisotropy constant K_2 is neglected, since it is small in YIG at room temperature. After a few algebraic steps, the effective potential for the two directions is

$$V_{\langle 100\rangle} = (V_{\parallel})_{\text{isotropic}} + 2K_1/M, \tag{15}$$

and

$$V_{\langle 110\rangle} = (V_{\parallel})_{\text{isotropic}} - K_1/2M \tag{16}$$

where $V_{\langle 100\rangle}$ is the effective potential for $\vec{H}_a \parallel \langle 100\rangle$ and $V_{\langle 110\rangle}$ is the effective potential for $\vec{H}_a \parallel \langle 110\rangle$.

Before applying the above analysis, we need to calculate the variations of M, D, and K_1 near the interface, since the effective potentials are a function of these parameters. The evaluation of these parameters at the interface is the subject matter of the next section.

III. CALCULATIONS OF MAGNETIC PARAMETERS IN THE DIFFUSION

In the region where the ion concentrations are uniform (as in pure YIG and GdGaG) the values of M, K_1, and D are obtained from published values. In the region near the YIG-GdGaG interface the ion concentrations are[1] spatially dependent and we need to estimate M, K_1, and D in order to apply the equation of motion *throughout* the film. The ion concentration profile has been measured[1] on CVD and LPE films of YIG.

The Y, Fe, Gd, and Ga concentrations were monitored by the peak-to-peak intensity of their respective $L_3M_{4,5}M_{4,5}$ (1740 eV), $L_3M_{2,3}M_{4,5}$ (650 eV), $N_{4,5}N_{6,7}N_{6,7}$ (138 eV), and $L_3M_{4,5}M_{4,5}$ (1070 eV) Auger transitions. The data were taken in multiplex mode while sputtering with 2-keV Ar ions incident at an angle of 70° from the sample normal. The etch rate was measured to be 3 Å per μ Å min/cm^2. The etch rate was measured by noting the elapsed time that it takes to completely remove the YIG film of a known thickness from the GdGaG substrate.

If the YIG-GdGaG interface were perfectly sharp, the Auger measurements would show a finite width of the order of 20 Å at the interface due to a variety of reasons: the sampling depth of the Auger electrons, an ion-induced mixed layer contributed by implantation effects, and surface roughness contributed either as grown film thickness variations or by sputter-induced variations. Sputter-induced roughness is due to differential sputtering from grain boundaries, different crystal orientations, density variations, etc.; it generally increases with the depth of material removed. The YIG films are single crystal with low dislocation density, so this contribution to interface width was not expected. Its absence was confirmed by measuring the interface width for different YIG film thicknesses. There was sample to sample variation of the interface width for the LPE films, but this variation was independent of YIG film thickness between 2500 Å and 6700 Å, and is believed due to variations in that thickness inside the 10–20-μm spot analyzed by the Auger spectrometer.

The ion-induced mixing at the bombarded surface occurs over a depth range of approximately the ion implant depth. For 2-keV Ar ions, this distance is expected to be on the order of 10–20 Å (small compared to the observed interfacial width).

The Auger sampling depth is determined by the electron mean free path in the material. This parameter is energy dependent; reasonable values for the Auger transitions used here are $\lambda_i = 18$, 10, 4, and 14 Å for Y, Fe, Gd, and Ga, respectively. The sampling depths will contribute to two phenomena—broadening of the interface width and the location of the observed point when each element is one half of its initial-final concentration difference. Both of these effects will be of the order of λ_i and therefore small compared to the observed interface widths. The LPE film profile in Fig. 1 shows one-half points at 140, 140, 142, and 138 min for Y, Fe, Gd, and Ga, respectively. The Gd is observed last, as expected from its short λ_i, the others do not show the expected sequence. However, the ion-induced mixing and film thickness variations may blur the expected sequencing.

The interface width is estimated by fitting the steep portion of each element interface profile with a straight line and extrapolating it to intercept the initial and final concentrations. The data in Table

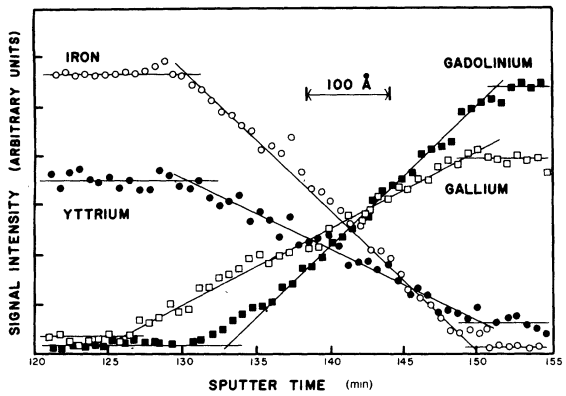

FIG. 1. Composition depth profile of a 2500-Å LPE YIG film on GGG; only the interfacial region is recorded here. Elemental concentration is inferred from the peak-to-peak heights of the 140-eV Gd, 703-eV Fe, 1060-eV Ga and 1745 eV-Y Auger transitions.

I shows roughly equal width for all the elements for LPE grown films. CVD films without anneal has a wider interface and after annealing, the CVD film shows pronounced interdiffusion of the Fe and Ga species.

Each positional point in the interface is designated by the chemical formula

$$Gd_XY_{3-X}Ga_YFe_{5-Y}O_{12}.$$

The values of X and Y are obtained by normalizing the vertical axis of Fig. 1 for each constituent so that in the region where the Fe and Y concentrations are constant $Y=X=0$ (YIG) and in the region where Gd and Ga are constant $X=3$, $Y=5$ (GGG). Distance is measured with respect to the point where the values of X and $Y=0$. Due to the resolution of the Auger Data, errors of 20–30 Å can result in initiating the zero-distance point. Distance is calibrated by sputtering away a film of known thickness, as shown in Fig. 1. Although it is well known that Y substitutes for Gd ions, the Ga ions may substitute for either the iron octahedral (a site) or tetrahedral (d site) sites. For a set of values of X and Y, the total moment M at a point is obtained by referring to the work of Maguire and Green[18] where M was measured as a function of Gd and Al impurities in YIG. Al and Ga reduce the iron moments by the approximate same amount.[19] In this assumption it is assumed that the bulk values of M can be directly transferred to a corresponding point in the interface for a given set of values of X and Y. M can also be estimated by assuming that for small values of Y, all of the Ga is substituted in the d site.[20] We have calculated M using both assumptions. We find that M is slightly dependent on the initial assumption made. However, K_1 is critically dependent on these two assumptions, since K_1 is strongly[21] dependent on the sublattice moments. The exchange parameter D is calculated in a random-phase approximation[13] and also using an improved approximation due to LeCraw and Walker.[14]

In a molecular-field approximation, the sublattice moments can be expressed as

$$M_a = N_a g\mu_\beta S B_{5/2}(g\mu_\beta S H_a/kT)\,, \tag{17}$$

$$M_d = N_d g\mu_\beta S B_{5/2}(g\mu_\beta S H_d/kT)\,, \tag{18}$$

$$M_c = N_c g\mu_\beta S B_{7/2}(g\mu_\beta S H_c/kT)\,, \tag{19}$$

where

$$N_a = N_a^{(0)}(1-\tfrac{1}{2}y_a)\,, \tag{20a}$$

$$N_d = N_d^{(0)}(1-\tfrac{1}{3}y_d)\,, \tag{20b}$$

$$N_c = N_c^{0}\tfrac{1}{3}x\,. \tag{20c}$$

N_a and N_d are the iron occupation numbers in the a and d sites. The amount of gallium per chemical formula unit found in the a and d sites are y_a and y_d, respectively. The total amount of gallium

TABLE I. Auger sputter-depth profile.

Film preparation	Thickness (Å)	Interface thickness (Å) Gd	Fe	Ga	Width[b]
LPE					
Sample 1	6700	330	340	240	290
Sample 2	6700	310	240	···	···
Acid etch from 7700 Å	2500	330	350	420	360
Acid etch from 7700 Å	2500	180	160	160	180
CVD					
Sample 1[a]	5600	200	630	430	150
Sample 2[a]	3700	490	1000	890	520
Sample 3	3700	520	610	570	550

[a]Annealed at 1200 °C.
[b]Width was measured by linear extrapolation.

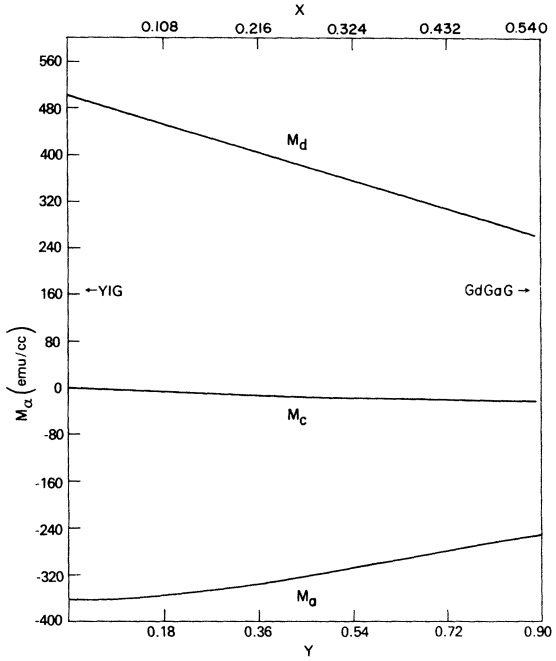

FIG. 2. Calculated sublattice magnetizations M_α are plotted as a function of Ga (Y) or Gd (X) concentrations at the interface. Point $X=Y=0$ corresponds to YIG, whereas $X=3$ and $Y=5$ to GdGaG. Sublattice magnetizations were calculated using Fig. 1 and the assumptions $M=M_a+M_d+M_c$ and $Y=Y_a+y_d$, where y_a and y_d are the amounts of Ga in the a and d sites, respectively.

in the iron sites is

$$Y=y_a+y_d\,. \tag{21}$$

N_c is the gadolinium occupation number in the c site. For no gallium or gadolinium impurities (pure YIG), for example,

$$N_a=N_a^{(0)}\,,$$

$$N_d=N_d^{(0)}\,,$$

$$N_c=0\,.$$

The molecular exchange fields at each site are defined as

$$H_a=\lambda_{aa}M_a+\lambda_{ad}M_d+\lambda_{ac}M_c\,, \tag{22}$$

$$H_d=\lambda_{da}M_a+\lambda_{dd}M_d+\lambda_{dc}M_c\,, \tag{23}$$

$$H_c=\lambda_{ca}M_a+\lambda_{cd}M_d+\lambda_{cc}M_c\,. \tag{24}$$

Since the M_α's are in units of emu/cm^3, the molecular-field exchange parameters $\lambda_{\alpha\beta}$ are dimensionless. $\lambda_{\alpha\beta}$ can be related to the nearest-neighbor spin-spin exchange interaction parameters, $(J_{ij})_{\rm nn}$. In order to identify which ions partake in the interaction, let $(J_{ij})_{\rm nn}\equiv J_{\alpha\beta}$. For example, λ_{aa} is related to $J_{aa'}$ by

$$\lambda_{aa}=2J_{aa'}z_a/N_a g^2\mu_B^2$$

where z_a is the number of iron nearest neighbors in the a site, and is equal to (assuming random distribution of gallium)

$$z_a=z_a^{(0)}(1-\tfrac{1}{2}y_a) \tag{25}$$

where $z_a^{(0)}$ is the value of z_a for *no* gallium impurities. However,

$$z_a/N_a=z_a^{(0)}/N_a^{(0)}\,.$$

Similarly,

$$z_d/N_d=z_d^{(0)}/N_d^{(0)}\,,$$

$$z_c/N_c=z_c^{(0)}/N_c^{(0)}\,.$$

This means that the molecular-field exchange parameters $\lambda_{\alpha\beta}$ in the iron sites can be taken to be constant in the diffusion region and equal to their respective bulk values in YIG. A similar conclusion applies to the c site. Finally, T in Eqs. (17)–(19) is the temperature and it is equal to 292 K, since our analysis applies only for ambient temperatures.

Equations (17)–(19) were used in an iterative procedure to solve for M_a, M_d, M_c, N_a, and N_d. The two constraining equations were

$$M=M_a+M_d+M_c\,,$$

$$Y=y_a+y_d$$

for one assumption. The values of M and Y are fixed at each point in the interface. Y and the corresponding value of X are obtained from Fig. 1 at a given point. For each set of values of X and Y there corresponds a value of M obtained in Ref. (18). Figure 2 shows a plot of M_a, M_d, and M_c versus Y or X (using the first assumption). The sign convention is that M_d is positive and in the opposite direction to both M_a and M_c, as expected. For the second assumption, all gallium goes to the d site, the two constraining equations are

$$y_d=Y,\quad y_a=0\,.$$

M, of course, is a variable to be determined in this type of assumption. Figure 3 shows the difference in calculated values of M_a and M_d using the two assumptions. The difference in M_c using the two assumptions is negligible. For both Figs. 2 and 3, the following set of values for the λ's were used[22]: $\lambda_{aa}=9433$, $\lambda_{ad}=14\,096$, $\lambda_{ac}=124$, $\lambda_{dd}=4489$, $\lambda_{dc}=1262$, $\lambda_{cd}=631$, and $\lambda_{cc}=31$. The total magnetization M is plotted as a function of distance for the two assumptions made in Fig. 4. We note although the iron and yttrium concentrations vanish within a distance of ~400 Å (see Fig. 1), M vanishes within a distance of only ~170 Å (see Fig. 4). Thus, the region of chemical diffusion of the

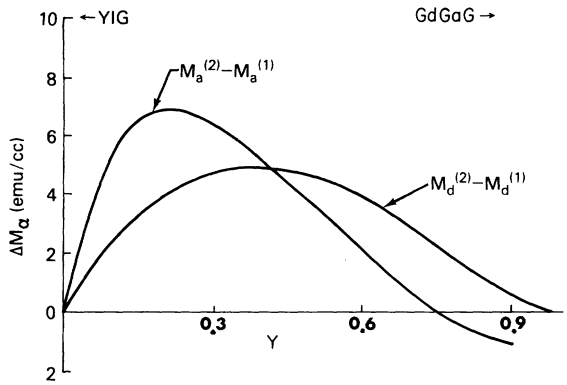

FIG. 3. Variation in magnetization of a and d sublattices caused by different assumptions regarding the distribution of gallium, between a and d sites. Superscript (1) refers to the assumption that all gallium goes to d size; superscript (2) refers to assumption discussed in the caption for Fig. 2.

ions is wider than the region in which magnetic order is sustained. Both assumptions give roughly the same variation of M with distance.

It is apparent from Figs. 2 and 4 that M reaches a compensation point at $Y\sim 0.95$ (distance ~170 Å) rather than a ferrimagnetic-paramagnetic transition point. Distance is measured from the point $Y=X=0$. We surmise that M should exhibit a net moment for

$$0.95<Y<5.0\,.$$

For values of Y greater than ~0.95, we would expect[20] the gallium to distribute among the two iron sites. Thus, invalidating one of our assumptions ($y_d=Y$). Also, for this range of Y and corresponding X values (see Fig. 1), there is no data on M to which we can refer. Thus, it becomes increasingly difficult to calculate the sublattice moments in this region. However, we can roughly estimate the magnetization in this range by linear extrapolation of M_a, M_d, and M_c in Fig. 2. We estimate a maximum moment of 10–20 emu/cm^3 at $Y\sim 1.5$ (distance ~280 Å). The paramagnetic point is reached at $Y\sim 2.0$, (distance ~320 Å) before the well-known paramagnetic point of $Y=5$ (GdGaG). Since the acoustic spin waves are vibrational modes of the total magnetization, and most of the total magnetization variation occurs for $Y<0.95$, most of the spin-wave scattering would occur within this region. These estimates apply only for ambient temperatures. At lower temperatures, the magnetization profile would be drastically different.

Let us calculate K_1 and D at the diffusion region. $K_2\approx 0$ for YIG at ambient temperatures, and we assume it to be also negligible in the diffusion region. The single-ion expression[12] for K_1 is given as

$$K_1 \simeq 26\,565[(1-\tfrac{1}{3}y_d)r_d - 0.063(1-\tfrac{1}{2}y_a)r_a]\ \text{erg/cm}^3\,, \qquad (26)$$

where

$$r_\alpha = -\frac{1+Q_\alpha-2Q_\alpha^2-2Q_\alpha^3+3Q_\alpha^4-Q_\alpha^5}{1+Q_\alpha+Q_\alpha^2+Q_\alpha^3+Q_\alpha^4+Q_\alpha^5}\,, \qquad (27)$$

$$Q_\alpha = \exp(-g\mu_B H_\alpha/kT), \quad \alpha=a,d\,. \qquad (28)$$

In the limit of $y_a=y_d=0$ (pure YIG) the above expression predicts the measured[23] temperature variation of K_1. The contribution to K_1 from the c site is small as estimated below.

$$K_{1c}\simeq 4300 r_c X\ \text{erg/cm}^3\,.$$

At ambient temperatures, the value[12] of r_c is -1.1×10^{-3} so that

$$-13<K_{1c}<0\ \ \text{erg/cm}^3\,.$$

This value is small compared to $K_1=-5200$ erg/cm^3 for bulk YIG. In calculating K_1 we used the values of sublattice moments obtained by the two assumptions. Substituting M_a, M_d, and M_c (obtained from the assumption $y_a=0$ and $y_d=Y$) into Eqs. (26)–(28), K_1 is determined at the interface. We find that for $Y\sim 0.95$ (distance ~150 Å) K_1 is reduced considerably, but still much higher than K_{1c}. Obviously, for $Y>0.95$, K_1 is small.

If we use the values of M_a, M_d, and M_c obtained from the first assumption ($Y=y_a+y_d$) to calculate K_1, we find that K_1 varies less than the other case. We cannot extend the calculations of K_1 beyond this point, since there is no measured value of M for impurities of $Y>1$ and $X>0.6$ in bulk YIG. However, we can roughly extrapolate from Fig. (5)

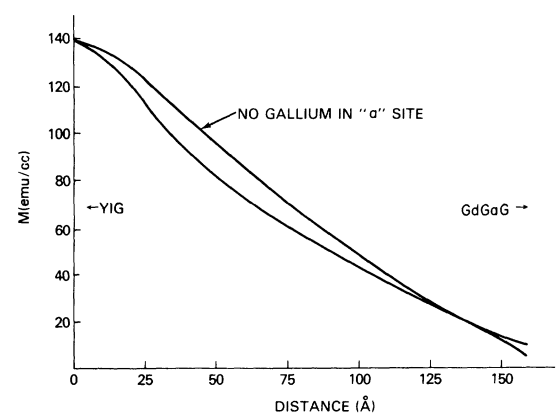

FIG. 4. Calculated total magnetization M is plotted as a function of distance at the interface for a LPE films. Assumptions described in Figs. 2 and 3 were used to calculate M.

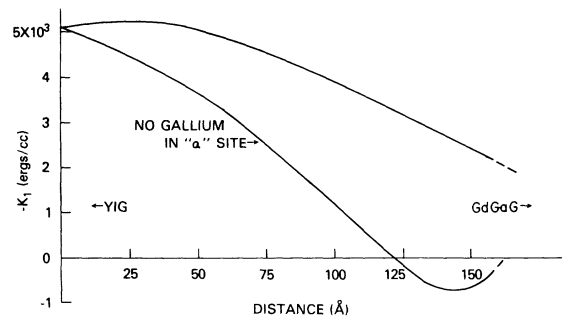

FIG. 5. Calculated cubic magnetic anisotropy parameter K_1 is plotted as a function of distance at the interface for LPE film. Assumptions described in Figs. 1 and 3 were used to calculate K_1.

that K_1 reaches zero at a distance of ~220 Å from the YIG boundary.

In the calculation of D we refer to the works of A. B. Harris,[13] and LeCraw and Walker.[14] If D is calculated in a random-phase approximation,[13] the expression for D is

$$D/l^2 = [M_a(12M_aJ_{aa'} + 5M_dJ_{ad} + 5M_cJ_{ac}) + M_d(2M_dJ_{dd'} + \tfrac{4}{3}M_cM_cJ_{dc}) + 2M_c^2J_{cc'}]/3732M\ \mathrm{cm}^{-1}, \quad (29)$$

where l is the lattice constant.

Also, Eq. (4) of Ref. 14 is used to calculate D. In this approximation,[14] the sublattice spin moments are proportional to the sublattice magnetizations. The contribution from the c site to the value of D is neglected, since the exchange couplings from this site to the iron sites are small. Using published[22] values of J_{ij}'s, and the sublattice magnetizations of Fig. 2, we find that the calculated value of D is not as sensitive as K_1 is to M_a, M_d, and M_c. We note that the calculation of LeCraw and Walker[14] yields an approximately constant value of D over the region of interest (see Fig. 6). For the other approximation[13] the values of D near $Y \sim 0.95$ appear to be improbable, since we would expect D to be small near the region where M vanishes for $Y \sim 2$ (the paramagnetic point).

In calculating M, K_1, and D we have referred to the Auger data of Fig. 1 which apply for a typical LPE film. The same analysis was applied also to CVD films.

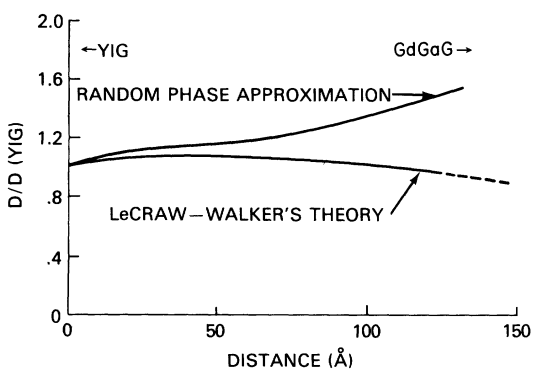

FIG. 6. Calculated exchange interaction parameter, D/D(YIG) is plotted as a function of distance at the interface for a LPE film.

IV. COMPARISON WITH EXPERIMENTS

As mentioned in previous sections, this analysis only applies at ambient temperatures. It may be possible to extend this analysis to other temperatures by substituting a given temperature value in the appropriate set of formulas of the previous sections. The analysis is the same for whatever temperature is chosen. We choose ambient temperature, since spin-wave data and total moment data[18] at that temperature are available for comparison.

A. Surface spin-wave excitations

We will first consider CVD films and then LPE films. Figure 7 shows the magnetization profile for two typical CVD films. We fitted the profiles to an analytical function such that the magnetization at a distance y from pure YIG is of the form of $\tanh(2y/\Gamma)$, where Γ is a measure of the width of the diffusion. For one profile $\Gamma \sim 600$ Å. For the other profile $\Gamma \sim 400$ Å. We expect the analytical fit to M to be reasonably good near the YIG boundary ($X = Y = 0$). For $M \to 0$, the fit is not as

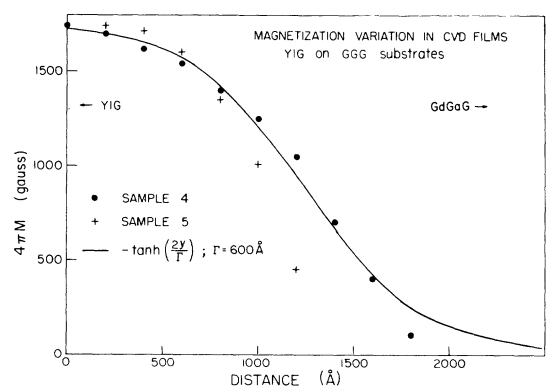

FIG. 7. Calculated total magnetization M is plotted as a function of distance at the interface for two CVD films. Calculated M is fitted to an analytical function of the form $\tanh(2y/\Gamma)$. The point $2y/\Gamma = 0$ corresponds roughly to the center of the interface.

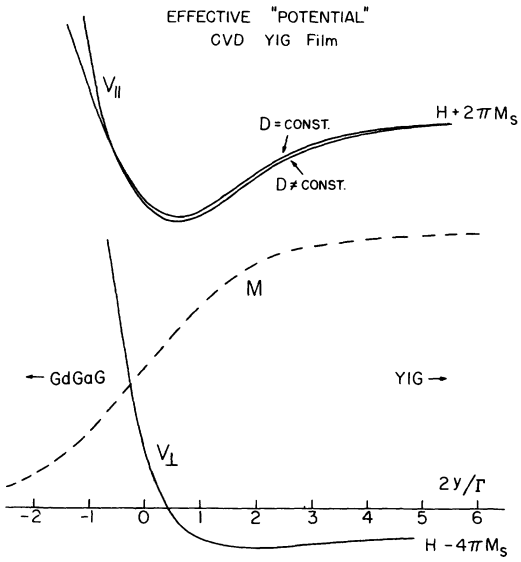

FIG. 8. Effective potentials $V_{\parallel}$ and $V_{\perp}$, for H parallel and perpendicular to the film plane. Analytical variation of M (see Fig. 7) is used to generate $V_{\parallel}$ and $V_{\perp}$.

good, since the calculated M approaches a compensation rather than a ferrimagnetic-paramagnetic transition point. The function $\tanh(2y/\Gamma)$ has a long tail for $y \to \pm\infty$. However, the region near $M \to 0$ is not crucial in the excitation of surface states as it will be demonstrated. The analytical function allows us to take second derivatives of M as is required in Eqs. (13) and (14). Let us now obtain the effective potential as defined in Eqs. (13) and (14) for H_a parallel and perpendicular to the film plane and for one profile ($\Gamma \sim 600$ Å) of M in Fig. 7.

In Fig. (8), the effective potentials $V_{\parallel}$ and $V_{\perp}$ are plotted as a function of distance near the interface. In the region where M is uniform, the resonance condition for the uniform resonance mode (Ω_u) is

$$\Omega_u \simeq H_a + 2\pi M_s$$

for H_a parallel to the film plane and

$$\Omega_u = H_a - 4\pi M_s$$

for H_a perpendicular to the film plane. We note that within the interface there is a potential well. For $\Omega > \Omega_u$ there exist volume spin-wave modes.[16] For $\Omega < \Omega_u$, there is a possibility for the excitation of a bound or localized spin-wave state.

It is noted that as $M \to 0$, $V_{\parallel}$ and $V_{\perp}$ increase rapidly. Since this part of the effective potential is energetically above the potential well, it plays a minor role in the excitation of a bound state. However, the steep rise in V can effect the resonance frequency of volume spin waves. Secondly, for localized state excitations the variation of K_1 is neglected, since this variation is too small to affect the depth of the potential well of Fig. 8. The variation in D, shown in Fig. 6, slightly modifies the potential well. Greater variations of D could be incorporated in the analysis by modifying the effective potential. The potential well depth below the uniform mode excitation is bigger for $V_{\parallel}$ than it is for $V_{\perp}$. This is due to the fact that for $V_{\parallel}$ a factor of $2\pi M$ is added to $(D/M)\ \partial^2 M/\partial y^2$ whereas a factor of $4\pi M$ is subtracted from $(D/M)\partial^2 M/\partial y^2$ for $V_{\perp}$. Thus, a shallower well is obtained for $V_{\perp}$.

Let us now determine whether or not a bound state exists for the two cases. For this problem, we can refer to numerous solutions to various potential well problems found in quantum-mechanics books.[24] Of particular interest is the solution to the Morse potential-well problem.[24] The Morse potential is of the form

$$V = C[\exp(-2\eta y) - 2\exp(-\eta y)]\,. \tag{30}$$

We can fit the above potential to $V_{\parallel}$ (see Fig. 9) if we take

$$C = 630, \quad \eta = 1.2/\Gamma\,.$$

The eigenvalue solution[24] to the Morse potential is

$$\Omega_u - \Omega_n = C[1 - \eta(n + \tfrac{1}{2})(D/C)^{1/2}]\,. \tag{31}$$

Taking into account a 10% variation of D at the interface (see Fig. 6), we determine that for $V_{\parallel}$ there is only *one* bound state ($n = 0$). The shift in effective frequency field is

$$\Omega_u - \Omega_{n=0} = 150 \text{ Oe}, \quad \Gamma \sim 400 \text{ Å}\,,$$

$$\Omega_u - \Omega_{n=0} = 235 \text{ Oe}, \quad \Gamma \sim 600 \text{ Å}\,.$$

Thus, the bound state ($n = 0$) can be excited for frequencies below the uniform mode at a fixed applied field. Alternatively, this mode resonates for fields above the main uniform mode line for a fixed frequency experiment. We conclude that

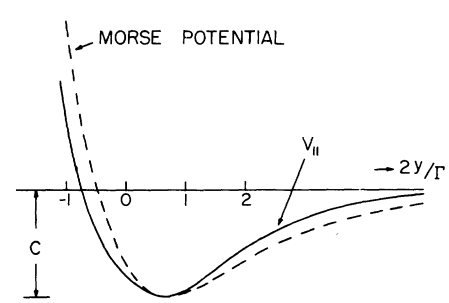

FIG. 9. Effective potential $V_{\parallel}$ for H_a parallel to the film plane is compared with a Morse-type potential. This potential applies for a CVD film of YIG (see Figs. 7 and 8).

this bound state is the surface spin-wave mode observed by Yu, Turk, and Wigen,[7] where it was found[7] to be localized at the interface between YIG and GdGaG. This surface spin-wave mode resonated[7] at a field of 115 Oe above the main line field. This is to be compared with our calculated values of 150 and 235 Oe for the two diffusion widths. With no other adjustable parameters, we find that there are no bound states excitation for H_a perpendicular to the film plane. This is in agreement with the observation[7] that the surface spin-wave mode was not observed for H_a perpendicular to the film plane.

As the angle of H_a is varied from in-plane resonance, the factor C or the well depth gets smaller. It can be seen from Eq. (31) that the difference in frequency between the bound state and the uniform mode will decrease until it reaches a value of zero. This means that at some oblique angle the uniform mode and the surface spin-wave mode will coalesce in agreement with previous data.[7]

For LPE films, we calculate *no* bound or localized state at room temperature, since the diffusion width is too narrow to support a bound state. This is in agreement with the ambient temperature results of Krebs and Vittoria[8] on LPE films.

B. Volume spin-wave modes

The main effect observed[4] in thin films (~0.40 μm) of CVD is the departure from the n^2 law by the resonant fields of the spin-wave modes (see Table II). The data in Table II was taken at 9.22 GHz, H_a parallel to the film plane, and at ambient temperature. A complete set of data on CVD films has been reported previously.[2,3,7] The departure from n^2 can be explained in terms of an infinite well where one side has a tapering with respect to the other. The width of the well increases with high-energy excitations (high n). For example, in our case a thickness of 4000 Å must be assumed for the $n=1$ spin-wave mode, and a thickness of 4080 Å must be assumed for the $n=8$ mode. Thus, it is clear that some sort of tapering of the type shown in Fig. 8 is needed in order to explain the departure from n^2 found in CVD films. Satisfactory theoretical[5,6] fits to the measured[3] departure in n^2 have been obtained by this approach. Auger data[1] confirms the validity of the assumption used in such calculations. A similar calculation on this point would be redundant and it would contribute no new physics.

No departure from n^2 was observed in LPE films of YIG for the spin-wave modes observed.[8,9] High n spin-wave mode intensities are too weak to be resolved by our spectrometer. We found that the intensities were dependent on the in-plane field direction of $\vec{H}_a$. The spin-wave intensity measured[3] in CVD films for the same (n) mode is a factor of 100 bigger than spin waves measured[8,9] in LPE films. Therefore, small anisotropic variations in intensities were not detected in CVD films.

TABLE II. Spin-wave resonance fields for CVD film of YIG.

n	H_n (Oe) experimental	H_n (Oe) Kittel theory [a]	Departure from n^2 law
1	5115	5115	0
2	4987	4986	+1
3	4770	4770	0
4	4475	4468	+7
5	4092	4080	+12
6	3615	3606	+9
7	3087	3045	+42
8	2610	2398	+212

[a]Dispersion law used to fit the X-band data was $H_n = 5158 - 43.12n^2$, $n \neq 0$; thickness $\simeq 0.4\ \mu$m.

The data[9] demonstrate a spin-wave intensity dependence on the in-plane angle of $\vec{H}_a$ which we attribute to the nonuniform distribution of K_1 at the interface. Let us first estimate the order of magnitude of the effect that a variation of K_1 can have on the spin-wave intensities. In order to estimate the effect of only K_1 variation, we assume, for the sake of argument, that K_1 varies at the interface while M and D are uniform. We will later discuss the effect of also having a varying M and D. Assuming an exponential variation for K_1 near the interface, the following differential equation is obtained for H_a parallel to the film plane

$$\frac{d^2m}{dy^2} + k^2 m \simeq \Delta e^{-y/\Gamma}, \tag{32}$$

where

$$Dk^2 = \Omega - (H_a + 2\pi M_s + 2K_1^{(0)}/M_s),$$
$$D\Delta = 2|K_1^{(0)}|/M_s; \quad \vec{H}_a \parallel \langle 100\rangle,$$
$$D\Delta = K_1^{(0)}/2M_s; \quad \vec{H}_a \parallel \langle 110\rangle.$$

M_s and $K_1^{(0)}$ are the saturation magnetization and magnetic anisotropy constants of pure YIG, respectively. Γ defines roughly the extent to which K_1 varies and for LPE films, $\Gamma \sim 150$ Å.

The series-expansion solution to Eq. (30) is

$$m = \bar{C}\left\{\cos ky + \sum_{s=1}^{\infty}\left[\Gamma^2\Delta\, e^{-y/\Gamma}\right]^s \times\left[\prod_{n=1}^{s}\left(\frac{n\cos ky + 2k\Gamma\sin ky}{n^2+4k^2\Gamma^2}\right)\right]\Big/ s!\right\}, \tag{33}$$

where k is a wave-vector constant. For LPE films

the factor $\Gamma^2\Delta \sim 0.06$ and, thus, to first order in $\Gamma^2\Delta$ the solution for m is

$$m \propto \cos ky + \frac{\Gamma^2\Delta(e^{-y/\Gamma})(\cos ky + 2k\Gamma \sin ky)}{1+4k^2\Gamma^2} \quad (34)$$

The above approximate solution corresponds to the Born-approximate solution to Eq. (30). For CVD films higher-order terms are needed, since the factor $\Gamma^2\Delta$ is much bigger. Let us now examine Eq. (32) for the case of LPE films. If $\Gamma \to 0$ (no variation of K_1), the solution of m is simply

$$m \propto \cos ky .$$

This is the zero-order solution to a uniform distribution of M, D, and K_1 and corresponds[4] to the solution for no spin pinning or no physical constraints at the two surfaces of the films. The wave vector is quantized[4] as

$$k = (\pi/d)n$$

where n is the spin-wave order number. For this case, the $n=0$ uniform precession mode couples to a uniform rf field in a FMR experiment. The first-order solution to Eq. (30) shows that spin waves are excited by the nonuniform distribution of K_1 at the interface. We find that, indeed, the spin-wave mode intensities are angular dependent for a given n and the ratio of the intensities for $\vec{H}_a \parallel \langle 110\rangle$ and $\vec{H}_a \parallel \langle 100\rangle$ is given as

$$I_n(\langle 110\rangle)/I_n(\langle 100\rangle) = \tfrac{1}{4}, \quad n \neq 0.$$

Thus, spin-wave intensities are weaker for $\vec{H}_a \parallel \langle 110\rangle$ for all values of n, except $n=0$. A variation in K_1 alone cannot explain the observed[9] anisotropy in spin-wave intensities. Alternation of intensities is observed[9] for the two directions of interest. It is observed that whereas $I_1(\langle 100\rangle) > I_1(\langle 110\rangle)$, $I_2(\langle 100\rangle) < I_2(\langle 110\rangle)$, and so on, (see Fig. 1 of Ref. 9). Variation in M alone and $K_1 = 0$ at the interface gives rise to an isotropic behavior in the intensities. It is possible to enhance or to reduce the dependence of the intensities on the two directions of H_a by allowing both K_1 and M to vary near the interface at different rates. However, no alternation of the type observed[9] in the intensities can be obtained by having K_1 and M varying at the interface. This means that besides varying M and K_1 a boundary condition at the YIG air side of the film *must* be introduced in order to fit the data of Ref. 9 in *totality*.

The same *exact* conclusions can be deduced, if we had assumed a calculational method[9] in which step variations of M and K_1 are assumed. Without loss of generalities, let us assume such a calculational method in attempting to fit in totality the spin-wave data of Fig. 1 in Ref. 9. After the fit, we will compare our fitting parameters with actual calculated variations of M, K_1, and D in Figs. 2–6. This calculation considers two magnetic layers coupled by electromagnetic boundary conditions. In one thick layer, a set of values of K_1 and M, corresponding to YIG values, is assumed while in the other thin layer, corresponding to the diffusion region, another adjustable set of values is taken. The parameter D is constant in both layers. Each layer is governed by a set of six equations similar to Eq. 4–9 in Ref. 25. The two layers are electromagnetically coupled by requiring the rf magnetic and electric fields, the magnetic moment and the spatial derivative of the magnetic moment to be continuous across the two layers. Since there are 6 internal rf fields to be solved in each layer, there results 12 coupled equations in terms of the internal rf fields. The method of calculating the FMR lineshape from this set of equations is shown in Ref. 25. The line

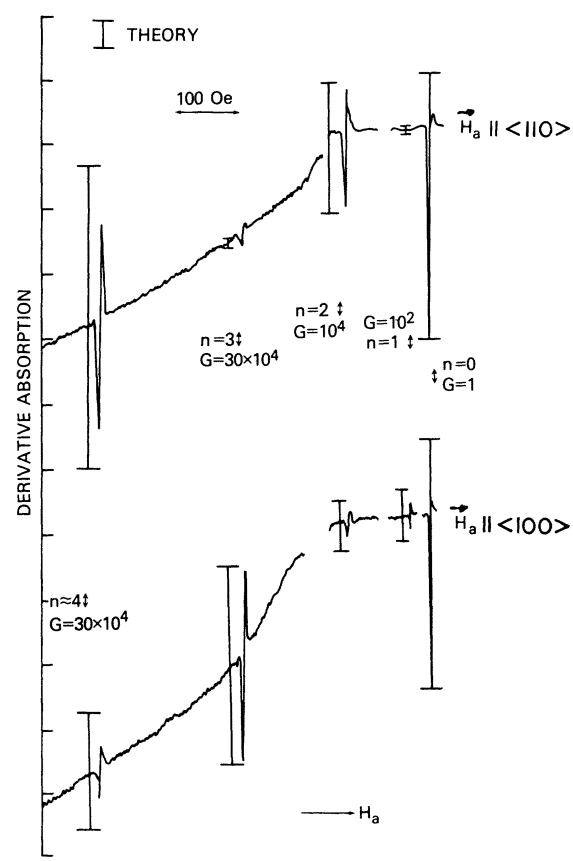

FIG. 10. Calculated and observed spin-wave spectra for H_a applied in the film (YIG) {100} plane. The resonant fields of the uniform mode are 2600 and 2486 Oe for $\vec{H}_a \parallel \langle 100\rangle$ and $\vec{H}_a \parallel \langle 110\rangle$, respectively. G indicates the gain setting for each spin-wave mode, and n is its order number. The slope in the baseline is due to the substrate (GdGaG) paramagnetic-resonance absorption.

shape of each spin-wave mode is calculated as a function of K_1, M, and the width (W) of the thin layer, and the YIG-air uniaxial surface anisotropy parameter, K_s. A boundary condition imposed at the other extreme surface does not modify significantly any of our results. After varying K_s, K_1, M, and W over considerable ranges a theoretical fit was obtained to the observed[9] spin-wave spectra (see Fig. 10). The value of K_s is 0.008 erg/cm^2. The values of M, $2K_1/M$, and W in the thinner layer were 129 emu/cm^3, −65 Oe, and $100 < W < 200$ Å. Let us discuss the implications of the above deduced parameters in terms of point-by-point calculations of M and K_1, (see Figs. 2–6). The actual calculated width of the diffusion, Fig. 4, is in remarkably good agreement with the value of W deduced by the above theoretical fit to the observed[9] spin-wave spectra. The deduced value of $2K_1/M = -65$ Oe implies that the fall-off rate of K_1 must be less than M. Indeed, this is the case if K_1 is calculated with the reasonable[20] assumption that gallium initially occupies only the d sites, see Fig. 5. Finally, the fact that only a small change of M is required to fit the spectra also implies a longer fall-off rate for M compared to K_1—in qualitative agreement with the previous conclusion. We conclude, that the deduced values of K_1, M, and W do have meaningful physical implications and, therefore, there is justification in the method we have used in fitting the spin-wave spectra. This is not surprising considering that the spin-wave wavelengths are considerably bigger than the thickness of the thinner layer of the above model.

V. CONCLUSIONS

Although qualitative arguments have been presented in the past in order to account for spin-wave excitation in films, we have presented *quantitative* arguments to explain the various types of excitation in YIG films. Our arguments apply to ambient temperatures excitations; however, our analysis is of sufficient generality to be applied for any temperatures. Our findings can be applied to other experimental situations found in thin film technologies.

We have confined our attention to one side of the YIG film (the YIG-GdGaG interface). It is clear that the YIG-air side plays a role in the excitation of volume spin-wave modes. For example, for LPE YIG we must introduce a surface anisotropy parameter of $K_s = -0.008$ erg/cm^2 in order to fit the spin-wave spectra.[9] The fact that this represents the smallest value of K_s measured in films, makes it possible to relate this value to some intrinsic property of the YIG-air boundary.

We would like to thank J. Mee, P. Besser, R. Henry, and H. Glass for making available to us the YIG films over the years; J. Murday for the Auger data; V. J. Folen, P. Lubitz, and G. T. Rado for helpful discussions.

[1]J. Murday, H. Lessoff, and C. Vittoria, Physica (Utr.) B 86, 1251 (1977).
[2]P. J. Besser, J. Appl. Phys. 42, 1570 (1971); M. Sparks, B. R. Tittman, J. E. Mee, and C. Newkirk, *ibid.* 40, 1518 (1969).
[3]S. Bhagat, H. Lessoff, C. Guenzer, and C. Vittoria, Phys. Status Solidi A 20, 731 (1973).
[4]C. Kittel, Phys. Rev. 110, 1295 (1958).
[5]C. S. Guenzer, H. Lessoff, and C. Vittoria, AIP Conf. Proc. 18, 1292 (1973).
[6]R. E. Dodd and L. K. Wilson, J. Appl. Phys. 45, 462 (1974).
[7]J. T. Yu, R. A. Turk, and P. E. Wigen, Phys. Rev. 11, 420 (1975), and references therein.
[8]J. Krebs and C. Vittoria, AIP Conf. Proc. 24, 486 (1974).
[9]C. Vittoria and H. Lessoff, Phys. Rev. Lett. 37, 53 (1976).
[10]M. Sparks, Phys. Rev. B 1, 3869 (1970); A. M. Portis, Appl. Phys. Lett. 2, 69 (1963); O. G. Rames, C. H. Wilts, Phys. Status Solidi B 79, 313 (1977).
[11]K. Yosida and M. Tachiki, Progr. Theor. Phys. 17, 331 (1957).
[12]W. P. Wolf, Phys. Rev. 108, 1152 (1957).
[13]A. B. Harris, Phys. Rev. 132, 2398 (1963).
[14]R. C. LeCraw and L. R. Walker, J. Appl. Phys. 32, 1675 (1961).
[15]L. Landau and E. Lifshitz, Z. Phys. 8, 153 (1935).
[16]A. M. Clogston, H. Suhl, L. R. Walker, and P. W. Anderson, J. Phys. Chem. Solids 1, 129 (1956).
[17]C. Vittoria and N. D. Wilsey, J. Appl. Phys. 45, 414 (1974).
[18]E. A. Maguire and J. J. Green, J. Appl. Phys. 33, 1373 (1962).
[19]G. R. Harrison and L. R. Hodges, J. Am. Ceram. Soc. 44, 214 (1961).
[20]S. Geller, J. Appl. Phys. 31, 305 (1960).
[21]V. J. Folen and G. T. Rado, J. Appl. Phys. 29, 4385 (1958).
[22]E. E. Anderson, Phys. Rev. 134, A1581 (1964). There is a slight spread in the published values of J_{ij}. We varied the values of J_{ij} within this allowed spread in order to satisfy the criteria of the iron occupation numbers and the proper temperature variation of M in YIG and GdIG.
[23]G. P. Rodrique, H. Meyer, and R. V. Jones, J. Appl. Phys. 31, 3765 (1960).
[24]See, for example, L. Landau and E. Lifshitz, *Quantum Mechanics Non-relativistic Theory* (Pergamon, Oxford, 1958), p. 71.
[25]G. C. Bailey and C. Vittoria, Phys. Rev. B 8, 3247 (1973).